

An RMS-DC Converter Based on the Dynamic Translinear Principle

J. Mulder, A. C. van der Woerd, W. A. Serdijn, and A. H. M. van Roermund

Abstract—The dynamic translinear principle can be regarded as an extension of the conventional, i.e., static, translinear principle. The dynamic translinear principle cannot only be used to realize linear filters, but also constitutes an interesting approach to the implementation of nonlinear differential equations. In this brief, as an example, a dynamic translinear realization of the nonlinear differential equation describing the rms-dc conversion function is designed, yielding a circuit with a high functional density. Measurement results of a prototype semicustom realization of the rms-dc converter show a good accuracy for crest factors up to ten and a cutoff frequency beyond 5 MHz for all input signal levels.

Index Terms—Bipolar analog integrated circuits, circuit synthesis, companding, continuous-time filters, nonlinear dynamic circuits, rms-dc conversion.

I. INTRODUCTION

TRANSLINEAR filters [1] (which are also called log-domain filters [2], companding current-mode filters [3], or exponential state-space filters [4]) are receiving increasing interest in literature, mainly due to their suitability for low-voltage applications. Translinear filters are based explicitly on the exponential behavior of the bipolar transistor or the MOS transistor operating in the subthreshold region. This class of circuits is instantaneously companding. The voltages in a translinear filter are logarithmically related to the currents, the principal carriers of information, which is advantageous in a low-voltage environment.

Translinear filters can be regarded as a generalization of the conventional, i.e., static, translinear principle [5]. By judiciously adding capacitances to the translinear loops, all kinds of frequency-dependent linear transfer functions can be realized. Since the dynamic translinear principle is an extension of the static translinear principle, translinear filters inherit the advantages of conventional translinear circuits. The main advantages are, first of all, a high functional density, which explains the extensive application of translinear circuits in neural networks, e.g., [6], and second, translinear circuits are theoretically process and temperature independent.

Next to these general characteristics of translinear circuits, translinear filters have some additional advantages with respect to other filter implementation techniques. First, only transistors and capacitors are required to realize a filter function. Especially in ultra low-power applications, where resistance values become too large for on-chip integration, this is a very important advantage.

Second, translinear filters can be implemented very elegantly in class AB. Hence, the currents swings can be much

larger than the quiescent currents. This increases the dynamic range without increasing the average power consumption.

Last, translinear filters are excellently tunable. Not just the cutoff frequency and the Q , but any parameter can be made (linearly) current controllable [7], which makes these filters attractive as programmable building blocks.

In literature, the dynamic translinear principle has been used mainly to implement filters, i.e., *linear differential equations*. However, conventional static translinear circuits are well-known for the wide variety of nonlinear functions they can implement. Obviously, the dynamic translinear principle can be applied just as well to the implementation of *nonlinear differential equations*, thus extending the applicability of the dynamic translinear principle.

A simple example of a nonlinear frequency-dependent transfer function is rms-dc conversion, which is a basic function used in many signal processing applications [8]. The rms-dc function is used in this brief to demonstrate the applicability of the dynamic translinear principle to the implementation of nonlinear differential equations.

Some other examples of functions described by nonlinear differential equations are mixer-filter combinations [9], oscillators [10], phase-locked loops (PLL's) [11], syllabic companding filters [12], and possibly even chaos.

In Section II, the dynamic translinear principle is explained from a current-mode point of view. The design of an rms-dc converter based on this principle is treated in Section III. Measurement results of a semicustom IC realization of the rms-dc converter are presented in Section IV.

II. DYNAMIC TRANSLINEAR PRINCIPLE

Both the conventional translinear principle and the dynamic translinear principle are based on the exponential law describing the large signal behavior of the bipolar transistor or the MOS transistor operating in the weak inversion region. The collector current I_C of a bipolar transistor is described by

$$I_C = I_s e^{V_{BE}/U_T} \quad (1)$$

where all symbols have their usual meaning.

This simple exponential model is accurate across a wide range of currents. A measurement of $g_m U_T / I_C$, where g_m is the small-signal transconductance, of an integrated minimum-sized NPN transistor is shown in Fig. 1. This dimensionless quantity $g_m U_T / I_C$ represents the slope of V_{BE} , normalized with respect to U_T , versus the logarithm of I_C , which should ideally equal one. The figure shows that the exponential model, (1), is valid across approximately seven decades of current. Thus, the translinear principle has a very solid foundation.

Manuscript received November 20, 1996; revised January 23, 1997.

The authors are with the Electronics Research Laboratory, Delft University of Technology, 2628 CD, Delft, The Netherlands.

Publisher Item Identifier S 0018-9200(97)04364-3.

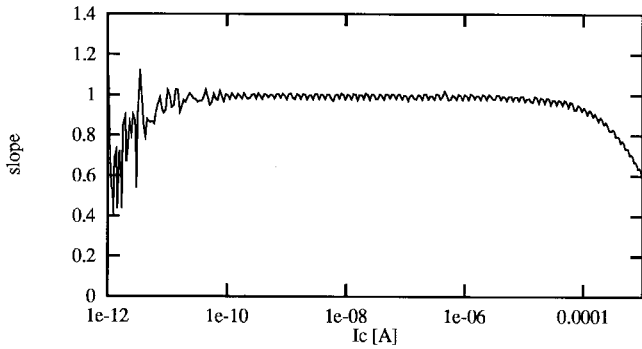


Fig. 1. Measurement of the slope of V_{BE} versus $\ln I_C$.

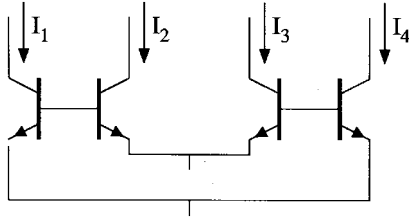


Fig. 2. Second-order translinear loop.

The exponential model is less accurate for MOS transistors in weak inversion, which behave exponentially across approximately four decades of drain current.

In Fig. 2, a basic four-transistor translinear loop is depicted. The conventional translinear principle states that this circuit can best be described in terms of the collector currents I_1 through I_4 . The translinear loop is thus described by a very simple equation

$$I_1 I_3 = I_2 I_4. \quad (2)$$

The dynamic extension of the translinear principle will be explained based on the generic subcircuit shown in Fig. 3. Just like the conventional translinear principle, the dynamic translinear principle can be explained best in terms of currents. By using a current-mode approach, no logarithmic functions, or other transcendental functions [4], have to be used to describe the circuits, thus increasing insight.

Another important advantage of a current-mode approach is the emphasis on the close relation between conventional and dynamic translinear circuits. As a consequence, existing theory regarding both analysis and synthesis of static translinear circuits, see e.g., [13], can be applied directly to analysis and synthesis of dynamic translinear circuits [1], [7].

Using the current-mode approach, the subcircuit shown in Fig. 3 is described in terms of the current I_{cap} flowing through the capacitance C . Note that the dc voltage source V_{const} does not affect I_{cap} . An expression for I_{cap} can be derived from the time derivative of (1). This yields an expression for the derivative \dot{V}_{BE} , where the dot represents differentiation with respect to time, of the base-emitter voltage. By applying the constitutive law of the capacitance, a current-mode expression for I_{cap} in terms of I_C is obtained

$$I_{cap} = CU_T \frac{\dot{I}_C}{I_C}. \quad (3)$$

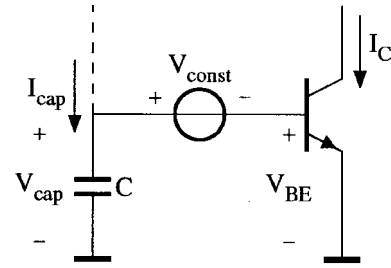


Fig. 3. Principle of dynamic translinear circuits.

This equation shows that I_{cap} is a nonlinear function of I_C and its time derivative \dot{I}_C .

A better insight in (3) is obtained by slightly rewriting it. Multiplying (3) by the (strictly positive) denominator I_C yields

$$CU_T \dot{I}_C = I_C I_{cap}. \quad (4)$$

This equation directly states the dynamic translinear principle: *A derivative of a current is equivalent to the product of that current and a capacitance current.* At this point, the conventional translinear principle comes into play, for, the product of currents on the right-hand side of (4) can be realized very elegantly by means of this principle. Thus, the implementation of (part of) a differential equation becomes equivalent to the implementation of a product of currents.

Equation (4) reveals another characteristic of dynamic translinear circuits. In general, translinear loops can be described by current-mode polynomials. The relation between these current-mode polynomials and the differential equations describing the transfer functions of dynamic translinear circuits is given by equations like (4). The right-hand side of (4) is implemented by (part of) a translinear loop. The left-hand side is part of the differential equation describing the transfer function to be realized. This mapping between a time derivative and a product of currents implies that the transfer function, i.e., the differential equation, becomes temperature dependent through U_T . Fortunately, this temperature dependence can be canceled easily by making (some of) the currents in the dynamic translinear circuit proportional to absolute temperature (PTAT) [2], [3].

III. DYNAMIC TRANSILINEAR RMS-DC CONVERSION

The translinear principle already plays a key role in conventional implementations of rms-dc converters [8], [14]. A well-known block schematic of an rms-dc converter is shown in Fig. 4. The system consists of two separate functions: a squarer-divider and a low-pass filter. The core of the implementation of the squarer-divider is a second-order translinear loop. This loop calculates the current I_{in}^2/I_{out} , where I_{in} and I_{out} are the input and output current of the rms-dc converter, respectively. The output current I_{out} equals the mean value of I_{in}^2/I_{out}

$$I_{out} = \left\langle \frac{I_{in}^2}{I_{out}} \right\rangle \quad (5)$$

where $\langle \dots \rangle$ represents the averaging operation, i.e., the low-pass filter shown in Fig. 4. By dividing I_{in}^2 by I_{out} , instead

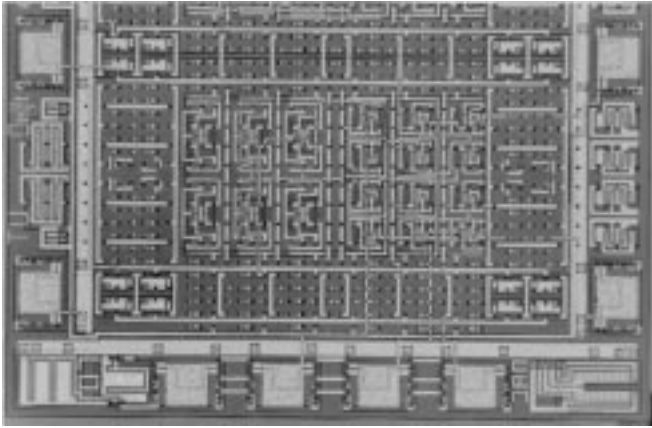


Fig. 7. Chip photograph.

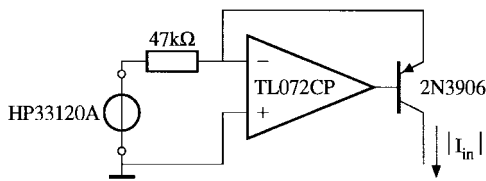


Fig. 8. Measurement setup.

respect to $|I_{in}|$. The problem can be solved by using a buffer amplifier. In Fig. 6, Q_7 is a simple implementation of this buffer. The other CC stage, transistor Q_8 , buffers the bases of Q_4 and Q_5 .

RMS-DC converters of second-order or higher can be designed by choosing a higher-order low-pass filter, instead of (6). Then, two or more capacitance currents will have to be introduced to eliminate the derivatives from the differential equation.

IV. MEASUREMENT RESULTS

The rms-dc converter was implemented on a semicustom IC in DIMES02, a 7-GHz bipolar process. A photograph of the circuit is shown in Fig. 7. The bias current sources I_o , shown in Fig. 6, are implemented by simple current mirrors.

Full-wave rectification and voltage-to-current conversion are accomplished by means of the setup shown in Fig. 8. An HP33120A Arbitrary Waveform Generator is programmed to supply a full-wave rectified output voltage, thus excluding the nonidealities of the alternative, an on-chip full-wave rectifier. The output voltage of the generator is converted to a current using a 47-k Ω resistor. The combination of a discrete op amp and a discrete PNP transistor is used as a current buffer. The output current of this buffer is the input current $|I_{in}|$ of the rms-dc converter. The output current of the rms-dc converter is measured across a 47-k Ω resistor. To facilitate a sufficient voltage range across the output resistor, a supply voltage of 4 V is used for the rms-dc converter, though its minimum supply voltage is only 2 V. The bias current I_o has a value of 85 μ A.

In Fig. 9, the relevant currents flowing in the rms-dc converter are shown. In this figure, C is 47 nF, which yields a cutoff frequency of 5.5 kHz. The input frequency is 12 kHz.

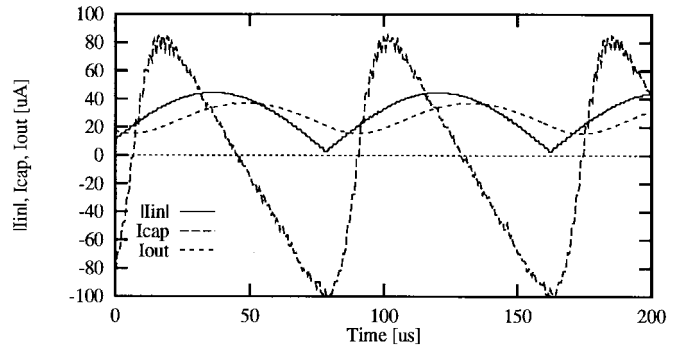
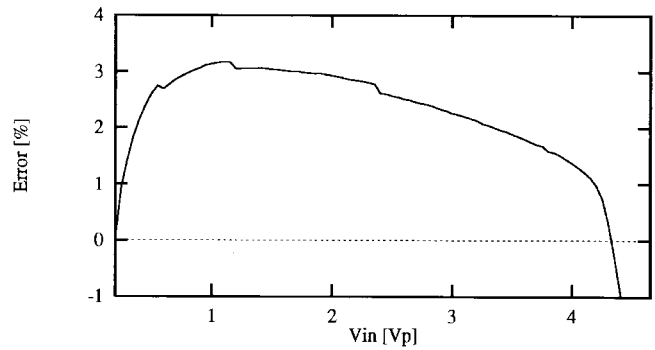

 Fig. 9. Currents $|I_{in}|$, I_{cap} , and I_{out} .


Fig. 10. Measured error versus input voltage.

The capacitance current is measured across a 4.7-k Ω resistor. The output voltage of the generator is 2 V_p. The figure illustrates the nonlinear relation between the capacitance current I_{cap} and the output current I_{out} . Further, it shows that I_{cap} can have much larger values than $|I_{in}|$ around the cutoff frequency.

For the next two measurements, a capacitance of 4.7 μ F is used, which yields a cutoff frequency of 55 Hz.

Fig. 10 shows the measured relative error for a rectified sine wave, at a frequency of 100 kHz, as a function of the amplitude. In this figure, V_{in} is the voltage supplied by the generator. For low values of V_{in} , the error curve is dominated by offsets in the measurement setup and the rms-dc converter, and by the limited bandwidth of the transistors at low current levels. For intermediate input levels, the curve shows a scaling error due to mismatches of the source and load resistors and of the transistors in the translinear loop. For values of V_{in} above 4 V, the output transistor of the rms-dc converter starts to saturate.

The error of the output of the rms-dc converter as a function of the frequency is shown in Fig. 11 for various values of the input voltage V_{in} . The -3 dB cutoff frequency could not be measured due to the limited frequency range (5 MHz) of the signal generator.

The worst-case waveform for an rms measurement is a rectangular pulse train, where all energy is contained in the peaks. The collector current of Q_3 takes its maximum value $I_{Q3,max}$ during the peaks of the input signal. The value of $I_{Q3,max}$ can be derived from (9) and is given by

$$I_{Q3,max} = CF^2 I_o \quad (10)$$

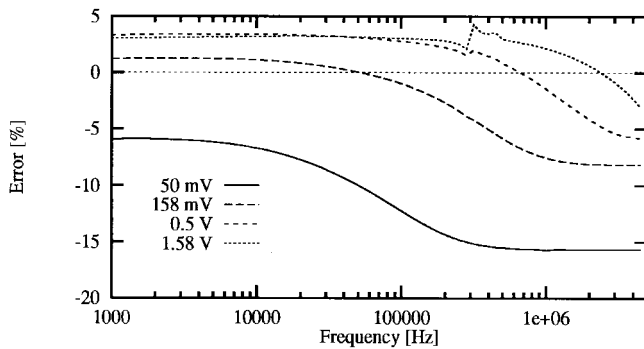


Fig. 11. Measured frequency response.

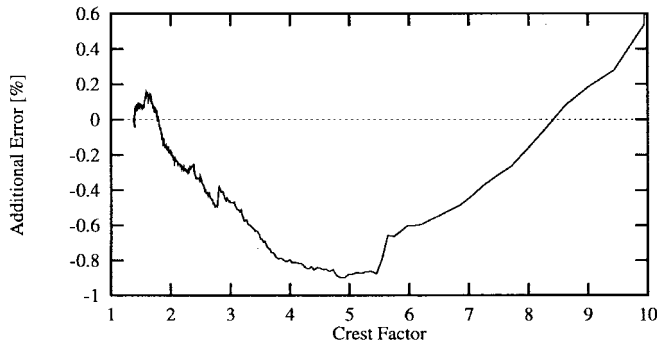


Fig. 12. Additional error versus crest factor.

where CF is the crest factor, the ratio between the peak value and the rms value of the input signal.

For high crest factors, $I_{Q3,max}$ becomes quite large, and as a consequence, transistor Q_3 , which is minimum sized, no longer behaves exponentially during the peaks, due to parasitic resistances and β_F high-current roll-off. Therefore, to perform a measurement of the error as a function of the crest factor, the current I_o is scaled down to 850 nA. The input resistor, shown in Fig. 8, and the output resistor are scaled up by a factor 100. The input voltage V_{in} switches between a bias level of 0.15 V and a certain peak voltage V_{peak} . The duty cycle and the peak voltage V_{peak} are varied to obtain different crest factors at a constant rms value of 0.4 V. The pulse width of the peak is constant and equals 200 μ s. Fig. 12 shows the measured additional error as a function of the crest factor. The error remains below 1% for crest factors up to ten.

V. CONCLUSION

Translinear filters exploit the exponential V-I characteristic of the bipolar transistor both to implement multiplications of

currents by means of the conventional translinear principle and to perform instantaneous companding. The dynamic translinear principle, a generalization of the conventional translinear principle, cannot only be used to realize *linear* filters, but can also be applied to implement *nonlinear* differential equations.

RMS-DC conversion is one example of an operation described by a nonlinear differential equation. The dynamic translinear principle was used to synthesize a completely translinear implementation.

To verify this new approach, the developed dynamic translinear rms-dc converter was realized on a semicustom IC. Measurements show a relative inaccuracy of several percent, mainly due to mismatch. The rms-dc converter has a bandwidth beyond 5 MHz and operates properly for crest factors up to ten.

REFERENCES

- [1] J. Mulder, A. C. v. d. Woerd, W. A. Serdijn, and A. H. M. v. Roermund, "General current-mode analysis method of translinear filters," *IEEE Trans. Circuits Syst.—I*, vol. 44, pp. 193–197, 1997.
- [2] R. W. Adams, "Filtering in the log domain," *63rd Convention A.E.S., LA*, preprint 1470, May 1979.
- [3] E. Seevinck, "Companding current-mode integrator: A new circuit principle for continuous-time monolithic filters," *Electron. Lett.*, vol. 26, no. 24, pp. 2046–2047, Nov. 1990.
- [4] D. R. Frey, "Exponential state space filters: A generic current mode design strategy," *IEEE Trans. Circuits Syst.—I*, vol. 43, pp. 34–42, Jan. 1996.
- [5] B. Gilbert, "Translinear circuits: A proposed classification," *Electron. Lett.*, vol. 11, no. 1, pp. 14–16, Jan. 1975.
- [6] A. G. Andreou and K. A. Boahen, "Translinear circuits in subthreshold MOS," *Analog Int. Circuits and Signal Processing*, no. 9, pp. 141–166, Apr. 1996.
- [7] J. Mulder, W. A. Serdijn, M. H. L. Kouwenhoven, A. C. van der Woerd, and A. H. M. van Roermund, "Dynamic translinear circuits—An overview," presented at *ISIC'97*, Singapore, 10–12 Sept. 1997.
- [8] C. Kitchin and L. Counts, "RMS to DC conversion application guide," in *Analog Devices*, 1983.
- [9] D. Frey, "Log domain filtering for RF applications," *IEEE J. Solid-State Circuits*, vol. 31, pp. 1468–1475, Oct. 1996.
- [10] W. A. Serdijn, J. Mulder, A. C. van der Woerd, and A. H. M. van Roermund, "A wide-tunable translinear second-order oscillator," in *Proc. IEEE ProRISC*, 1996, pp. 295–298.
- [11] W. A. Serdijn, J. Mulder, A. C. van der Woerd, and A. H. M. van Roermund, "Design of dynamic translinear phaselock loops," submitted to *Int. J. Analog Integrated Circuits, Signal Processing*, 1997.
- [12] J. Mulder, W. A. Serdijn, A. C. v. d. Woerd, and A. H. M. v. Roermund, "An instantaneous and syllabic companding translinear filter," Accepted for publication, *IEEE Trans. Circuits Syst.—I*, 1997.
- [13] E. Seevinck, *Analysis and Synthesis of Translinear Integrated Circuits*. Amsterdam: Elsevier, 1988.
- [14] B. Gilbert, "Translinear circuits—25 years on—Part III: Developments," *Electron. Eng.*, pp. 51–56, Oct. 1993.
- [15] ———, "Novel technique for R.M.S.-D.C. conversion based on the difference of squares," *Electron. Lett.*, vol. 11, no. 8, pp. 181–182, Apr. 1975.